

# Thermospheric parameters' long-term variations over the period including the 24/25 solar cycle minimum. Whether the CO<sub>2</sub> increase effects are seen?

Andrey V. Mikhailov<sup>a,b</sup>, Loredana Perrone<sup>b,\*</sup>, Anatoly A. Nusinov<sup>c</sup>

<sup>a</sup> Pushkov Institute of Terrestrial Magnetism, Ionosphere and Radio Wave Propagation (IZMIRAN), Troitsk, Moscow, 108840, Russia

<sup>b</sup> Istituto Nazionale di Geofisica e Vulcanologia (INGV), Roma, 00143, Italy

<sup>c</sup> Fedorov Institute of Applied Geophysics (IAG), Moscow, 129128, Russia

## ARTICLE INFO

### Keywords:

Long-term trends  
Climate change

## ABSTRACT

The CO<sub>2</sub> concentration has been increasing for more than five decades reaching ~29 % at present with respect to the pre-industrial era. The largest CO<sub>2</sub> cooling effects in the thermosphere are predicted for solar minimum conditions. A comparison of solar minima in 1954/1964 to the recent one in 2019 was used to check at the quantitative level the theoretical predictions and the validity of the CO<sub>2</sub> cooling hypothesis. June monthly median noontime ionospheric observations at Moscow, Rome, and Slough/Chilton were used to infer neutral gas density  $\rho$ , exospheric temperature  $T_{\text{ex}}$ , height of the F<sub>2</sub>-layer maximum  $h_m F_2$ , and total solar EUV flux for the (1954–2020) period. Solar and geomagnetic activity was shown to explain ~99 % of the whole variability in the retrieved neutral gas density and  $T_{\text{ex}}$  during the (1958–2020) period resulting in statistically insignificant residual linear trends. A comparison of 1954/1964 to 2019 solar minima does not confirm the theoretically predicted decrease of ~21 % in  $\rho$ , ~15 K in  $T_{\text{ex}}$ , and ~7 km in  $h_m F_2$  related to a 29 % increase of the CO<sub>2</sub> abundance. The main conclusion: despite continuous CO<sub>2</sub> increase in the Earth's atmosphere long-term variations of thermospheric parameters are controlled by solar and geomagnetic activity.

## 1. Introduction

Thirty years have passed since issuing of the first publications by Roble and Dickinson (1989) and Rishbeth (1990) devoted to possible impact of greenhouse gases (mainly CO<sub>2</sub>) on the Earth's upper atmosphere. Along with these model predictions Rishbeth (1977) had stressed: "long-term changes can only be reliably detected over intervals of time that greatly exceed the 11-year solar cycle. The present ionospheric record is only marginally adequate for such studies". Long-term changes of the upper atmosphere parameters related to the CO<sub>2</sub> increase should result in cooling and subsiding of the thermosphere i.e. in a decrease of neutral gas density at fixed heights and shrinking of the ionosphere. In accordance with the predictions negative trends have been found in electron concentration and in the height of F<sub>2</sub>-layer (Ulich and Turunen, 1997; Bremer, 1998, 2001, 2008; Jarvis et al., 1998; Sharma et al., 1999; Danilov, 2006; Laštovicka et al., 2012; Mielich and Bremer, 2013; Danilov and Konstantinova, 2013; Laštovicka, 2013, 2017; Roininen et al., 2015) as well as in thermospheric temperature and neutral gas density according to satellite drag and Incoherent Scatter Radar (ISR) observations (Zhang et al., 2011; Zhang and Holt,

2013; Oliver et al., 2014; Ogawa et al., 2014; Emmert, 2015a,b and the references therein). First-principle (physical) model simulations have also confirmed the expected cooling effects in the upper atmosphere related to the CO<sub>2</sub> increase (Qian et al., 2008, 2011; Cnossen, 2014; Solomon et al., 2018, 2019). Along with this obvious contradictions with observations have been found (Perrone and Mikhailov, 2016).

The CO<sub>2</sub> increase in the Earth's atmosphere (<https://www.co2.earth>) is going on with the rate of ~5.5 % per decade (Qian et al., 2017) for the period longer than 5 decades and it would be interesting to check predicted changes in the ionospheric and thermospheric parameters. However there are not many possibilities to do this. A way to check the upper atmosphere cooling may provide satellite drag observations (Keating et al., 2000; Emmert et al., 2004; Marcos et al., 2005; Emmert, 2015a and references therein) which do manifest a decrease of neutral gas density at 400 km with the rate depending on solar activity. The last estimate by Emmert (2015a) without any separation on solar activity gave the average decrease in  $\rho$  of  $-2.0 \pm 0.5$  % per decade over the 1967–2005 period. Fitting any empirical thermospheric model to the observed neutral gas variations in principle it is possible to estimate a trend in the exospheric temperature,  $T_{\text{ex}}$  and this approach gave a

\* Corresponding author.

E-mail address: [loredana.perrone@ingv.it](mailto:loredana.perrone@ingv.it) (L. Perrone).

<https://doi.org/10.1016/j.jastp.2021.105736>

Received 14 December 2020; Received in revised form 1 August 2021; Accepted 10 August 2021

Available online 13 August 2021

1364-6826/© 2021 The Authors.

Published by Elsevier Ltd.

This is an open access article under the CC BY-NC-ND license

(<http://creativecommons.org/licenses/by-nc-nd/4.0/>).

decrease of  $\sim -1\text{K}$  per decade (Emmert, 2015a, Table 2). However one should bear in mind that neutral gas density at thermospheric heights depends both on neutral composition (mainly atomic oxygen) and exospheric temperature,  $T_{\text{ex}}$ . Data on atomic oxygen were absent in that analysis and the observed decrease in neutral density was formally prescribed to a decrease in  $T_{\text{ex}}$ . Our analysis (Perrone and Mikhailov, 2019) has not revealed any statistically significant decrease in the atomic oxygen abundance over the period of some decades in agreement with the Emmert's conclusion (2015a) that neutral density decrease is due to a decrease in  $T_{\text{ex}}$ . The inferred neutral temperature decrease may be compared to the predicted cooling of the thermosphere due to the  $\text{CO}_2$  concentration increase. Under a double  $\text{CO}_2$  increase scenario the  $T_{\text{ex}}$  decrease is  $\sim 50\text{K}$  (Rishbeth 1990; Rishbeth and Roble, 1992). Today we have a 29 %  $\text{CO}_2$  increase in the Earth's atmosphere with respect to the 1960 level (317 ppm) (<https://www.co2.earth>). Assuming a linear dependence one may expect a 14.5 K decrease in  $T_{\text{ex}}$ . Under the observed rate of  $\text{CO}_2$  increase 5.5 % per decade (Qian et al., 2017) the cooling process has started  $\sim 53$  years ago resulting in the cooling rate of  $\sim 2.7\text{K}$  per decade. This coincides with the Whole Atmosphere Community Climate Model-eXtended (WACCM-X) model simulation cooling rate of 2.8 K per decade obtained by Solomon et al. (2018) for solar minimum conditions. Similar model simulations under solar maximum gave the cooling rate of 1.8K per decade (Solomon et al., 2019). Therefore the average cooling rate of 2.3 K per decade results in  $\sim 12\text{K}$  cooling of the thermosphere over 53 years. On the other hand the retrieved from satellite drag observations cooling rate of  $\sim 1\text{K}$  per decade (Emmert, 2015a) gives only a  $\sim 5\text{K}$   $T_{\text{ex}}$  decrease over the same period. Therefore the inferred from  $\rho$  observations thermospheric cooling is by two times less than is expected from the 29 %  $\text{CO}_2$  increase in the Earth's atmosphere.

Another source of information on thermospheric temperature long-term variations is Incoherent Scatter Radar (ISR) observations. The ISR method routinely provides ion temperature  $T_i$  which is identified with neutral one,  $T_n$ . Such  $T_n$  trends are by an order of magnitude larger than satellite drag observations provide:  $-60\text{K/decade}$  at 350 km for daytime hours at Saint Santin/Nancay (Donaldson et al., 2010),  $-10$  to  $-15\text{K/decade}$  at  $F_2$ -layer heights for day-time hours at Tromso (Ogawa et al., 2014), and  $-20\text{K/decade}$  at 350 km for daytime hours at Millstone Hill (Zhang and Holt, 2013). The unreality of such  $T_n$  trends was stressed repeatedly (e.g. Emmert, 2015a,b, Emmert et al., 2004, 2021; Solomon et al., 2018). The situation was discussed by Perrone and Mikhailov (2017, 2018a) and it was suggested that the effect can be due to the ISR method itself based on a fixed model of ion composition and such ISR observations might be not appropriate for long-term trend analyses.

Of course, the best opportunity for long-term trend analyses presents ground-based ionospheric sounding observations. Using the same method of ionospheric sounding the world-wide ionosonde network has provided round o'clock ionospheric observations for some decades and some European stations have been working for more than 70 years. Naturally, ionosonde observations are widely used for long-term trend analyses, the results may be found in review papers (Danilov, 2012; Laštovička et al., 2012; Laštovička, 2013, 2017; Danilov and Konstantinova, 2020).

Electron concentration in the ionosphere depends on many aeronomic parameters such as: solar EUV, neutral composition and temperature, neutral winds and electric fields and this is not easy to separate and remove these contributions to reveal the effect solely related to the  $\text{CO}_2$  increase. The situation is simpler with mid-latitude daytime E-region which is controlled by photo-chemical processes following the classic Chapman (1931) theory. However even in this case very different estimations of  $f_0E$  long-term trends may be found in the literature, for references see (Danilov & Konstantinova, 2018, 2020). Our analysis (Mikhailov et al., 2017) of June noontime monthly median  $f_0E$  long-term variations at three European stations Rome, Juliusruh, Slough/Chilton has shown the existence of a rising phase from the middle of

1960s– $\sim 1985$  and a falling phase after 1985. A close similarity (even in details) between 11-year running mean smoothed  $(f_0E_{\text{ave}})_{11\text{y}}$  and sunspot number  $(R_{12})_{11\text{y}}$  variations with the correlation coefficient of 0.996 ( $R^2 = 0.992$ ) tells us that more than 99 % of the whole  $(f_0E_{\text{ave}})_{11\text{y}}$  variability is explained by solar activity i.e. the Sun is the only source of  $f_0E$  long-term variations at least for summer noontime conditions.

The majority of ionospheric trend analyses are devoted to  $F_2$ -layer parameter long-term variations. However this is not that easy to demonstrate the  $f_0F_2$  changes related to the  $\text{CO}_2$  increase in the Earth's atmosphere. Apart from the obvious dependence of  $f_0F_2$  on solar cycle which may be removed by a regression with any solar index (sunspot numbers  $R$ ,  $F_{10.7}$ , or  $E_{10.7}$ ) electron concentration in the  $F_2$ -region depends on geomagnetic activity but indirectly via atomic oxygen and thermospheric winds, both strongly affecting  $f_0F_2$ . A direct addition of geomagnetic indices such as  $A_p$  (either monthly or annually or smoothed) to the regression does not improve the regression accuracy for  $f_0F_2$  and this was earlier noted in some publications. This is due to the formation mechanism of mid-latitude daytime  $F_2$ -layer. On one hand increased geomagnetic activity decreases the atomic oxygen concentration at F-region heights decreasing  $N_mF_2$  which is  $\sim [O]^{4/3}$  (Mikhailov et al., 1995), on the other hand elevated auroral heating damps the northward thermospheric wind increasing by this way  $N_mF_2$ . Thus two processes work oppositely compensating each other to a great extent. However geomagnetic activity effects are clearly seen in the retrieved atomic oxygen abundance (Perrone and Mikhailov, 2019) and in the meridional thermospheric wind long-term variations (Mikhailov and Perrone, 2018).

The absence of a standard method to remove the effects of geomagnetic activity from  $f_0F_2$  long-term variations results in different  $f_0F_2$  trends inferred for the same period but with different methods (Laštovička et al., 2006). Further, without removal of geomagnetic activity effects the  $f_0F_2$  trends depend on the period chosen for the analysis. Fig. 1 gives  $\delta f_0F_2 = f_0F_{2\text{obs}}/f_0F_{2\text{reg}}$  long-term variations for Moscow and Slough/Chilton obtained after the  $f_0F_{2\text{obs}}$  regression with 3-month  $F_{10.7}$  – a standard step to remove solar cycle variations from observed monthly  $f_0F_2$  (e.g. Perrone and Mikhailov, 2016). The residual  $\delta f_0F_2$  manifest both year-to-year and long-term variations (see polynomial approximation) with rising and falling phases not related to 11-year solar cycles. By 11-year smoothing of  $\delta f_0F_2$  and  $A_p$  indices it is possible to remove these variations (Mikhailov et al., 2002, also Laštovička et al., 2006) to obtain insignificant residual  $f_0F_2$  trend. However this is not a generally accepted method and usually the problem of removing geomagnetic activity effects from  $f_0F_2$  long-term variations is not discussed in trend analyses. But in this case the resultant  $f_0F_2$  trends depend on the selected time period. Trends estimated over the years including the rising phase (before 1975–1980) will be positive while they will be negative for the period after 1975. Depending on the contribution of the rising and falling phases to the analyzed period trends will be different for different selected time intervals. Obviously, that this effect has nothing common with the continuous  $\text{CO}_2$  increase in the Earth's atmosphere (Fig. 1, bottom panel) which is the main concern of our analysis.

WACCM-X model simulations by Solomon et al. (2018, 2019) predict an  $N_mF_2$  decrease of 1.2 % (0.6 % for  $f_0F_2$ ) per decade related to the  $\text{CO}_2$  increase both for solar minimum and maximum. This gives a  $\sim 3\%$   $f_0F_2$  decrease over the period of five decades. Bearing in mind the  $\delta f_0F_2$  scatter (Fig. 1) with the standard deviation of 5–6% this 3 %  $f_0F_2$  decrease related to the 29 %  $\text{CO}_2$  increase hardly can be reliably detected. Thus available methods of  $f_0F_2$  long-term trend analyses cannot be used to check at the quantitative level the predicted changes in  $f_0F_2$  related to the  $\text{CO}_2$  increase.

Nevertheless, excellent ground-based ionospheric observations can be utilized for such verification. With our recently developed method by Perrone and Mikhailov (2018b) it is possible to retrieve from routine  $f_0F_2$  and  $f_0F_1$  observations a consistent set of aeronomic parameters responsible for the formation of daytime mid-latitude F-region. The list

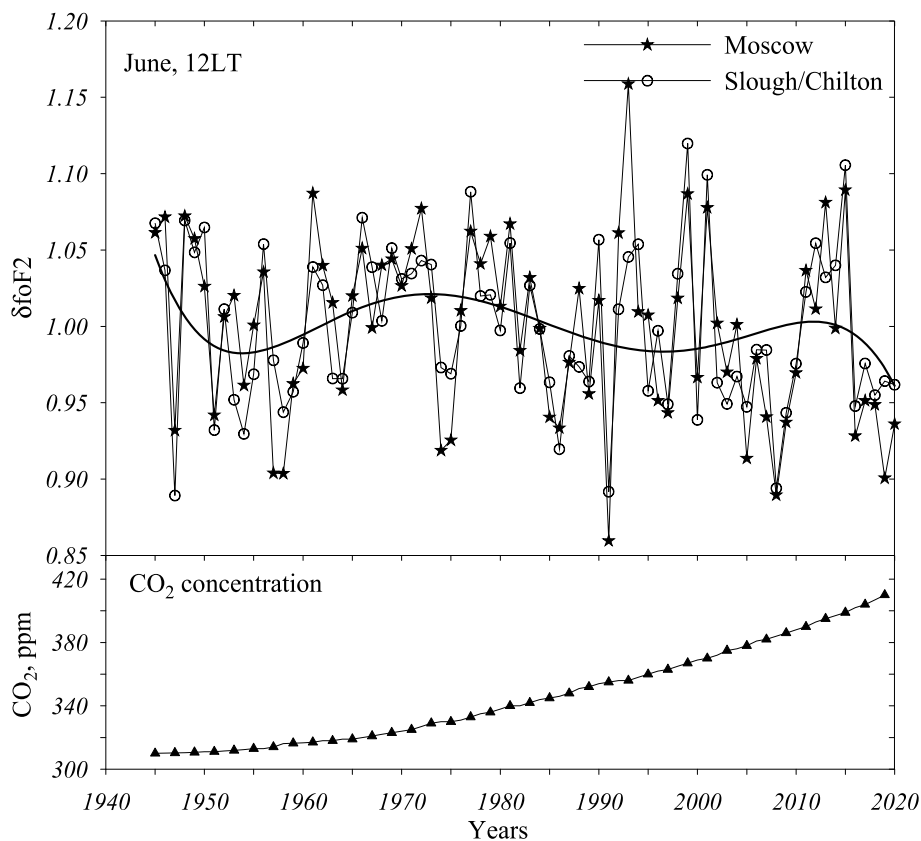


**Fig. 1.** June  $\delta f_oF_2 = f_oF_{2\text{obs}}/f_oF_{2\text{reg}}$  long-term variations at Moscow and Slough/Chilton along with the polynomial approximation illustrating different phases in these variations. Observed  $\text{CO}_2$  abundance in the Earth's atmosphere is given in the bottom panel.

of retrieved parameters includes: neutral composition ( $\text{O}$ ,  $\text{O}_2$ ,  $\text{N}_2$ ) and  $T_{\text{ex}}$ , vertical plasma drift mainly related to thermospheric winds, and the total solar EUV flux with  $\lambda \leq 1050 \text{ \AA}$ . The height of  $F_2$ -layer maximum,  $h_mF_2$  is also specified during fitting of observed  $N_mF_2$ .

According to satellite drag observations (Emmert, 2015a, also references therein) and model simulations neutral gas density trends are larger under solar minimum. WACCM-X model simulations by Solomon et al. (2018) for solar minimum conditions ( $F_{10.7} = 70$  and  $K_p = 0.3$ ) predict a decrease of 2.8K per decade for  $T_{\text{ex}}$ , 3.9 % per decade for neutral gas density at 400 km, and 1.3 km per decade for  $h_mF_2$ . Therefore one may expect a  $\sim 15 \text{ K}$  decrease in  $T_{\text{ex}}$ , a  $\sim 21 \%$  decrease in neutral gas density and a  $\sim 7 \text{ km}$  decrease in  $h_mF_2$  over the period of 53 years mentioned earlier. These are quite noticeable variations which should be seen in the retrieved parameters for solar minimum conditions.

Available ionospheric observations (at least at Moscow) cover seven solar minima from 1954 to 2019. The 1954 and 1964 minima corresponding to the period with low  $\text{CO}_2$  abundance (Fig. 1) may be considered as reference ones while the 2019 minimum corresponds to present day  $\text{CO}_2$  concentration with 414 ppm in the Earth's atmosphere. Therefore the retrieved  $T_{\text{ex}}$ ,  $h_mF_2$ , and  $\rho$  should demonstrate the effect of 29 %  $\text{CO}_2$  increase over the (1954/1964–2020) period. The aim of the undertaken analysis is to check whether the retrieved from ionospheric observations thermospheric parameter variations confirm model predictions under solar minimum conditions when the effects of  $\text{CO}_2$  increase should be the largest according to model simulations.

## 2. Observations, method, and results

The method by Perrone and Mikhailov (2018b) used in our analysis has two versions: a general one which may be used for any daytime conditions when  $f_oF_2$  and five plasma frequencies at 180 km height

( $f_{p180}$ ) at (10,11,12,13,14) LT are available, and a version when instead of  $f_{p180}$  five  $f_oF_1$  values are used. Plasma frequencies  $f_{p180}$  read from automatically scaled  $f_p(h)$  profiles are available only for the last two decades at the best while we need historical observations when only  $f_oF_1$  were available.  $F_1$ -layer is systematically present on ionograms only in summer, for this reason June observations were used for our analysis. Due to closeness of  $f_oF_1$  to  $f_oF_2$  under solar minimum conditions and intensive Es in summer automatic scaling turns out to be not very efficient and  $f_oF_1$  data are often absent at some stations for June 2019–2020. Three European stations Moscow (55.5°N; 37.3°E), Rome (41.9°N; 12.5°E), and Slough/Chilton (51.5°N; 359.4°E) with available June  $f_oF_2$  and  $f_oF_1$  observations over the whole period were selected for our analysis. Manual ionogram scaling was applied in some cases. A new recently developed model of solar EUV by Nusinov et al. (2021) is used as a starting EUV flux value in the retrieval process.

Table 1 gives monthly and 3-month  $F_{10.7}$  as well as monthly Ap and HL $\alpha$  (composite) along with noontime monthly median  $f_oF_2$  and  $f_oF_1$  values for June under seven solar minima. June  $f_oF_1$  observations are not available at Rome and Slough for 1954.

Table 1 gives that  $F_{10.7}$  indices were low  $\sim 70$  for all solar minima. But geomagnetic activity manifests a rising phase from 1954 to 1976 and a falling phase after 1976. This is similar to smoothed  $\delta f_oF_2$  variations shown in Fig. 1. In accordance with close  $F_{10.7}$  for all solar minima monthly median  $f_oF_2$ , and  $f_oF_1$  also demonstrate small inter-minimum variations. Observed (composite) HL $\alpha$  (Machol et al., 2019) being an indicator of the total solar EUV flux responsible for the ionization of the F-region also manifests very small inter-minimum variations.

The method by Perrone and Mikhailov (2018b) was applied to observed June noontime monthly median  $f_oF_2$ , and  $f_oF_1$  for the (1954–2020) period to retrieve aeronomic parameters responsible for the formation of mid-latitude daytime  $F_2$ -layer, in particular:  $h_mF_2$ ,  $T_{\text{ex}}$  and neutral gas density ( $\rho$ ) at 300 km. The variations of these parameters

**Table 1**

Solar, geomagnetic activity indices and the intensity of monthly median composite HL $\alpha$  for June along with noontime monthly median  $f_oF_2$  and  $f_oF_1$  for years of solar minimum.

Parameter	1954	1964	1976	1986	1996	2008	2019
$F_{10.7\text{mon}}$	67.3	69.0	70.6	67.6	69.6	65.9	68.1
$F_{3\text{mon}}$	67.7	68.5	69.6	70.1	70.3	66.7	68.8
$Ap_{\text{mon}}$ , nT	5.8	8.6	9.7	8.4	5.3	6.7	4.3
$HL\alpha \times 10^{11}$ , ph/cm <sup>2</sup> s	3.73	3.68	3.75	3.69	3.79	3.64	3.67
Moscow							
$f_oF_2$ , MHz	5.1	5.1	5.4	5.0	5.1	4.7	4.8
$f_oF_1$ , MHz	4.20	4.30	4.20	4.20	4.20	4.10	4.14
Rome							
$f_oF_2$ , MHz		5.5	5.6	5.2	5.3	5.1	5.1
$f_oF_1$ , MHz		4.45	4.40	4.37	4.37	4.23	4.30
Slough/Chilton							
$f_oF_2$ , MHz		4.9	5.1	4.7	5.1	4.5	4.9
$f_oF_1$ , MHz		4.32	4.35	4.25	4.30	4.24	4.28

**Table 2**

Correlation coefficients, R along with confidence intervals between the retrieved and approximated with (1) aeronomic parameter variations. Second lines – R<sup>2</sup> parameter.

Parameter	Moscow	Rome	Slough/Chilton
$\rho$	0.994 ± 0.005	0.993 ± 0.005	0.996 ± 0.004
	0.988	0.986	0.992
$T_{\text{ex}}$	0.994 ± 0.005	0.994 ± 0.005	0.994 ± 0.004
	0.988	0.988	0.988
$h_mF_2$	0.970 ± 0.024	0.950 ± 0.040	0.982 ± 0.014
	0.941	0.902	0.964

may be compared to model predictions by Solomon et al. (2018) for solar minimum conditions. The 300 km height (rather than 400 km usually used in satellite drag analyses) is used to avoid possible contribution of He which is essential at 400 km under solar minimum, while the retrieved neutral gas density includes only three neutral species - O, O<sub>2</sub>, and N<sub>2</sub>.

At first let us consider  $\rho$ ,  $T_{\text{ex}}$ , and  $h_mF_2$  long-term variations using (1958–2020) years to check whether statistically significant linear trends exist and after we will analyze inter-minimum variations for years given in Table 1. Although June  $f_oF_2$  and  $f_oF_1$  observations are available at Moscow since 1946 we use the same (1958–2020) period to compare trends at the three stations.

Solar and geomagnetic activity effects should be removed as much as possible from the retrieved parameters to analyze the residual variations. A comparison of various solar activity indices (Perrone and Mikhailov, 2017) has shown that 3-month averaged  $F_{10.7}$  ( $F_{3\text{mon}}$ ) can be applied for long-term trend analyses. June monthly Ap indices were used in the regression to remove geomagnetic activity effects. The final regression may be written as follows

$$P = b_0 + b_1 \times F_{3\text{mon}} + b_2 \times Ap \quad (1)$$

Fig. 2 (as an example) gives retrieved and calculated with the regression (1) aeronomic parameters as well as their ratios to estimate the residual long-term linear trends.

Fig. 2 indicates a good correlation between the retrieved and approximated with the regression (1) aeronomic parameter long-term variations (left panels) resulting in the insignificant residual trends (right panels). Only  $\delta h_mF_2$  and  $\delta \rho$  residual trends at Slough/Chilton are significant at the 95 % confidence level.

Table 2 summarizes the correlation coefficients between the retrieved and approximated variations as well as R<sup>2</sup> for three aeronomic parameters at the three stations. R<sup>2</sup> gives the percent of variability explained with the regression (1).

Table 2 shows that due to large correlations coefficients the R<sup>2</sup>

parameters are large as well. This means that solar ( $F_{10.7 \text{ 3mon}}$ ) and monthly Ap indices practically totally describe the inferred  $\rho$ ,  $T_{\text{ex}}$ , and  $h_mF_2$  long-term variations. The largest approximation accuracy takes place for neutral gas density - around 99 % of the whole variability is explained by solar and geomagnetic activity. Similar result manifests  $T_{\text{ex}}$  with ~99 % of explained variability. The least approximation accuracy the regression (1) demonstrates for  $h_mF_2$  - from 90 % at Rome to 96 % at Slough/Chilton. This may be attributed to a strong  $h_mF_2$  dependence on vertical plasma drift related to thermospheric winds. This drift demonstrates by itself long-term variations as this was shown by Mikhailov and Perrone (2018). The obtained results show that practically no space is left for the CO<sub>2</sub> contribution. For instance, a 1–2% of unexplained  $\rho$  variability is much less than can be expected from Solomon et al. (2018, 2019) model predictions:  $(3.9 + 1.7)/2 = 2.8$  % per decade  $\times$  5.3 decades = 14.8 %.

The largest thermospheric effects of the CO<sub>2</sub> increase are expected under solar minimum conditions. Let us consider inter-minimum changes of the retrieved  $T_{\text{ex}}$ ,  $\rho$ , and  $h_mF_2$  for solar minima given in Table 1. The retrieved parameters were reduced to  $F_{10.7} = 70$  and  $Ap = 3$  nT to be compared to Solomon et al. (2018) model simulation results. The regression (1) may be used for this reduction. The results for three stations are given in Table 3.

The observed  $F_{10.7}$  and Ap (Table 1) are close to  $F_{10.7} = 70$  and  $Ap = 3$  nT therefore the reduced values do not strongly differ from the initial ones. Ratios of the reduced to  $F_{10.7} = 70$  and  $Ap = 3$  nT neutral gas density  $\rho$ ,  $T_{\text{ex}}$  and  $h_mF_2$  for the 2019 minimum to the reference solar minima (1954 for Moscow and 1964 for Rome and Slough/Chilton) do not show the predicted decrease of ~21 % (3.9 % per decade  $\times$  5.3 decades) in  $\rho$ , ~15 K (2.8 K  $\times$  5.3 decades) in  $T_{\text{ex}}$ , and ~7 km (1.3 km  $\times$  5.3 decades) in  $h_mF_2$  related to a 29 % increase in the CO<sub>2</sub> abundance. Linear trends for these ratios calculated over all years of solar minimum are statistically absolutely insignificant. Therefore, the conducted analysis does not confirm the predicted decrease of aeronomic parameters related to a 29 % increase in the CO<sub>2</sub> abundance over the (1954/1964–2019) period.

### 3. Discussion

The CO<sub>2</sub> increase is going on with the rate of ~5.5 % per decade (Qian et al., 2017) and by now we have a 29 % increase in the CO<sub>2</sub> abundance with respect to the (1954–1964) period. The hypothesis of the upper atmosphere cooling by CO<sub>2</sub> requires a confirmation however practically this is not easy to do. At present the only experimental way to check the hypothesis at the quantitative level is to use satellite drag observations (Emmert, 2015a and references therein). According to model simulations by Solomon et al. (2018) the largest effect of the CO<sub>2</sub> increase is expected under solar minimum conditions, in particular a decrease of ~21 % in neutral gas density and a ~15K in exospheric temperature are predicted with the present day concentration of CO<sub>2</sub> in the Earth's atmosphere. Such changes should be seen in satellite drag observations. However the recent analysis by Emmert (2015a) gave very modest variations (see Introduction) both in neutral gas density and in  $T_{\text{ex}}$ . In the present paper using our recently developed method (Perrone and Mikhailov, 2018b) the thermospheric parameters have been retrieved from ionospheric observations over the period including two pre-industrial solar minima in 1954 and 1964 in a comparison to the recent solar minimum in 2019. However this comparison does not manifest any statistically significant changes as an expected reaction to a 29 % increase of the CO<sub>2</sub> concentration in the Earth's atmosphere. Of course, as with any indirect method (the satellite drag method to estimate  $\rho$  variations is also an indirect one) it is always valid a question – whether the applied method is correct?

Our method was tested with CHAMP/STAR neutral gas density observations (Perrone and Mikhailov, 2018b) and it was shown that the method provided statistically significant better results in a comparison to modern empirical thermospheric models. A comparison with Swarm

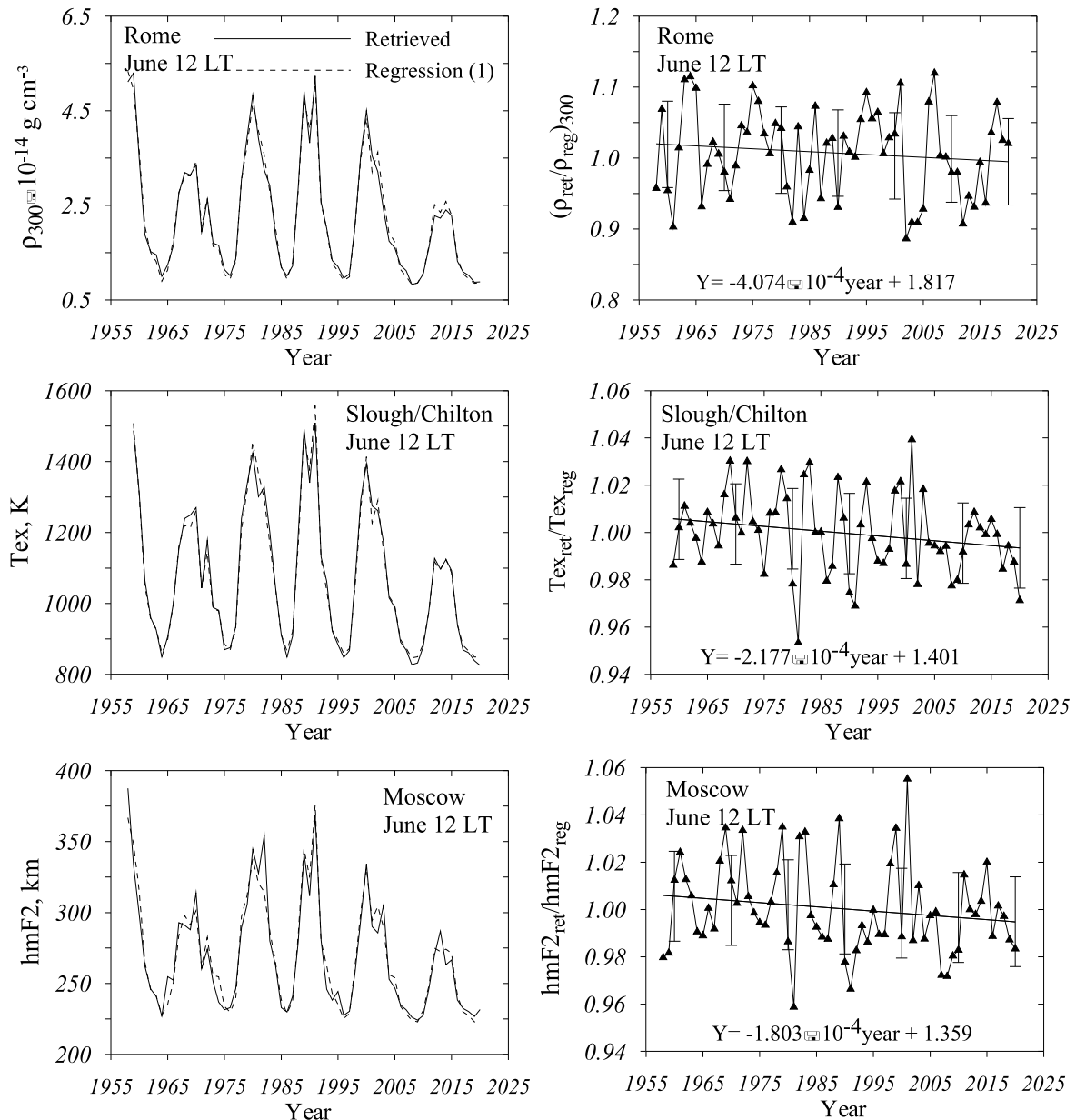


Fig. 2. Left panels – retrieved and obtained with the regression (1) neutral gas density at 300 km,  $T_{ex}$ , and  $h_m F_2$ . Right panels – ratios of the retrieved to regression values along with linear trends estimated over the whole period. Error bars correspond to  $\pm$  one standard deviation. The residual linear trends given in the bottom of right panels are statistically insignificant.

Table 3

Inter-minimum variations of the retrieved  $\rho_{300}$ ,  $T_{ex}$ , and  $h_m F_2$  at the three stations. Values reduced to  $F_{10.7} = 70$  and  $A_p = 3$  nT are given in brackets.

Parameters	1954	1964	1976	1986	1996	2008	2019
<b>Moscow</b>							
$\rho_{300} \times 10^{-14}$ , g cm $^{-3}$	0.861 (0.874)	0.929 (0.867)	1.033 (0.913)	1.004 (0.897)	0.924 (0.872)	0.815 (0.838)	0.875 (0.885)
$T_{ex}$ , K	815 (817)	838 (829)	848 (831)	842 (827)	835 (827)	809 (812)	825 (826)
$h_m F_2$ , km	227 (225)	227 (222)	233 (225)	230 (224)	228 (225)	226 (224)	227 (226)
<b>Rome</b>							
$\rho_{300} \times 10^{-14}$ , g cm $^{-3}$		1.000 (0.972)	1.015 (0.940)	1.009 (0.936)	0.959 (0.921)	0.827 (0.875)	0.877 (0.895)
$T_{ex}$ , K		826 (817)	837 (820)	834 (819)	822 (814)	800 (803)	815 (816)
$h_m F_2$ , km		230 (221)	233 (222)	233 (223)	228 (224)	231 (227)	228 (227)
<b>Slough/Chilton</b>							
$\rho_{300} \times 10^{-14}$ , g cm $^{-3}$		0.969 (0.926)	1.087 (0.988)	0.947 (0.866)	0.984 (0.939)	0.848 (0.886)	0.889 (0.904)
$T_{ex}$ , K		849 (839)	875 (857)	849 (833)	847 (839)	828 (831)	839 (840)
$h_m F_2$ , km		227 (218)	232 (220)	229 (219)	229 (224)	225 (220)	228 (226)

neutral density observations was used to explain the post-storm neutral density decrease in the thermosphere (Mikhailov and Perrone, 2020). Millstone Hill ISR noontime  $h_m F_2$  observations in 2000–2016 have been used to test the method (Perrone et al., 2020). The retrieved  $h_m F_2$  values demonstrated a standard deviation close to the expected inaccuracy of  $h_m F_2$  determination. A comparison of the retrieved EUV to the observed EUV one and to the EUVAC (Richards et al., 1994) empirical model provides an absolutely independent check of the method as the observed and model EUV values have nothing common with the retrieval process.

Due to Solar Radiation and Climate Experiment (SORCE) mission and the Thermosphere, Mesosphere, Ionosphere, Energetic, and Dynamics (TIMED) mission daily EUV (100–1200) Å observations (Woods et al., 2018) (<http://lasp.colorado.edu/lisird/>) are available since 2002. On the other hand, HL $\alpha$  is known to be a good proxy for solar UV radiation (Nusinov and Katyushina, 1994; Chamberlin et al., 2007). This was checked again using EUV (100–1200) Å (Woods et al., 2018) observations. Fig. 3 (left panel) gives such a comparison. June monthly median observed EUV are compared to monthly median HL $\alpha$  (Machol et al., 2019) variations. The correlation coefficient between two variations is  $0.995 \pm 0.009$  which is significant at the 99.9 % significance level. This allows us to compare the retrieved total EUV to HL $\alpha$  and to the EUVAC (Richards et al., 1994) model for the whole (1958–2020) analyzed period (Fig. 3, right panel).

The correlation coefficient between the retrieved EUV and HL $\alpha$  variations is  $0.978 \pm 0.018$  being significant at the 99.9 % confidence level according to Student criterion (Fig. 3, right panel). A coincidence is seen even in details – notice two-hump maxima in the even solar cycles. A comparison with the EUVAC model gives the correlation coefficient  $0.987 \pm 0.011$  which is also significant at the 99.9 % confidence level. All this tells us that the method by Perrone & Mikhailov, (2018b) does work and provides reasonable results.

In accordance with our concept long-term variations of thermospheric parameters are due to long-term variations of solar and geomagnetic activity. After the deepest for the whole history of ionospheric observations solar minimum in 2008/2009 with monthly  $F_{10.7} = 65.9$  in June and 65.7 in July 2008 one can hardly expect a new deeper solar minimum, anyway the recent 2019 solar minimum manifests larger monthly  $F_{10.7}$  (Table 1). Therefore the thermosphere and ionosphere just cannot further fall down and one should expect if not a growth but at least a stabilization of long-term variations at some level bearing in mind that we have entered into the period of low solar activity (<http://www.wdcb.ru/stp/data/solar.act/csa/Cycles%20of%20Solar%20Activity.en.pdf>).

Fig. 1 gives falling and rising phases in  $f_0 F_2$  long-term variations which manifest the corresponding variations of thermospheric

parameters. A falling phase took place until the middle of 1950s followed by a rising phase until the middle of 1970s. After this took place a prolonged falling phase until 2008–2009 which coincided with the industrial era and the CO<sub>2</sub> increase in the Earth's atmosphere. So after 2009 one may expect a new rising phase in thermospheric and ionospheric parameter long-term variations. Indeed, a recent extended analysis by Emmert et al. (2021, their Fig. 4), indicates no visible difference in annual mean neutral gas density comparing the last two solar minima in 2008 and 2019.

Problems with  $f_0 F_2$  linear trends after the inclusion of last observations have been mentioned in recent publications (De Harro Barbas and Ellias, 2019; Danilov & Konstantinova, 2019) and they have been attributed to peculiarities with the solar EUV versus  $F_{10.7}$  index dependence in the solar cycle 24. Laštovicka (2019) has discussed changes in relationships among solar indices. He has found that the dependence of Mg II (Viereck et al., 2001) versus  $F_{10.7}$  has become steeper in 1996–2014 compared to the previous time period indicating in his opinion changes of the relationship between solar proxies and EUV ionizing radiation.

Daytime mid-latitude ionospheric  $F_2$ -layer manifests the intensity of solar incident EUV radiation and the state of the surrounding thermosphere - neutral composition, temperature, and winds. Therefore, if everything is correct with the solar EUV versus  $F_{10.7}$  dependence then under continuously increasing CO<sub>2</sub> in the Earth's atmosphere changes or absence of negative trends in the upper atmosphere parameters should raise questions to the CO<sub>2</sub> cooling concept – whether it really works? Anyway the results of our analysis do not indicate any noticeable trends in the retrieved thermospheric parameters over the (1954–2019) period including a 29 % increase of the CO<sub>2</sub> abundance.

The EUV versus solar activity index dependence for the whole (1958–2020) period and separately for solar cycles 23 and 24 may be checked using HL $\alpha$  (Machol et al., 2019) data. By analogy with the EUVAC model (Richards et al., 1994) a half sum of 3-month and June monthly  $F_{10.7}$  ( $F_{0.5}$ ) was used as an index of solar activity (Fig. 4). The height of solar cycles 23 and 24 was different (the cycle 24 was lower) so June  $F_{0.5}$  indices were also different. Therefore for the purity of a comparison only years with  $F_{0.5} < 127$  (the maximal  $F_{0.5}$  value in the cycle 24) in both cycles were used in Fig. 4 (right panel).

Fig. 4 (left panel) indicates a good relationship between HL $\alpha$  and  $F_{0.5}$  with the correlation coefficient  $0.984 \pm 0.0132$  which is significant at the 99.9 % confidence level. Parameter  $R^2 = 0.968$  tells us that  $F_{0.5}$  explains ~97 % of the whole HL $\alpha$  variability i.e. no significant residual trend is expected in HL $\alpha$  long-term variations after removing of the solar cycle dependence. Bearing in mind a close HL $\alpha$  relationship with other lines in the solar EUV spectrum this conclusion is valid for the total

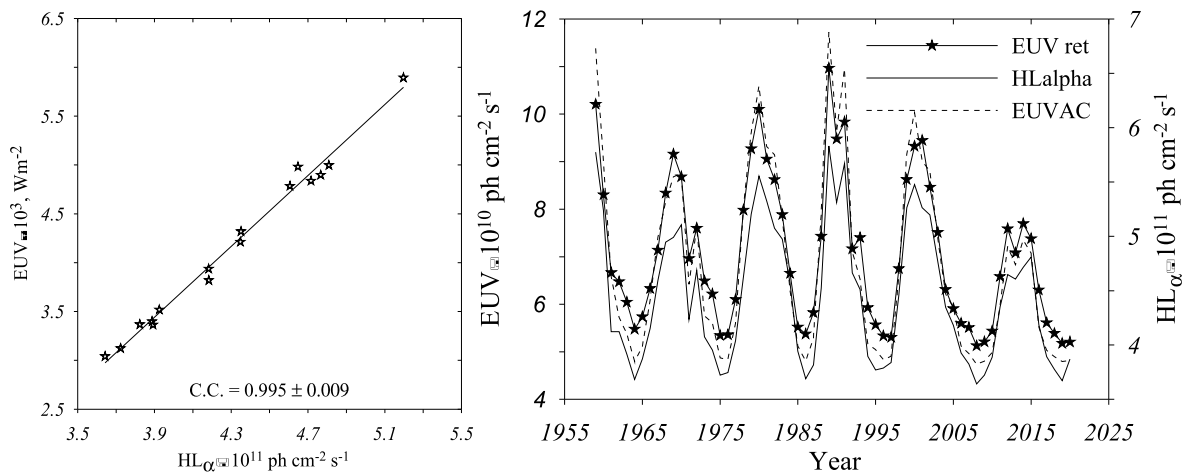
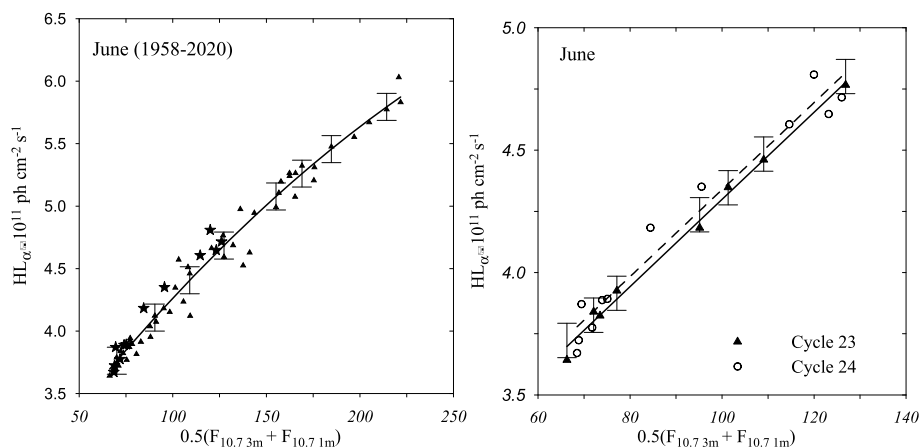


Fig. 3. Observed June monthly median total EUV (100–1200) Å versus composite HL $\alpha$  (left panel), solid line – a linear regression. Right panel gives a comparison of June monthly median retrieved EUV flux to composite HL $\alpha$  and EUVAC model variations for the whole (1958–2020) period.



**Fig. 4.** June composite  $HL\alpha$  versus  $F_{0.5}$  for the whole (1958–2020) period (left panel) and separately for solar cycles 23 and 24 (right panel) are given. Asterisks in the left panel correspond to solar cycle 24. Error bars -  $\pm$  standard deviations. Solid and dashed lines are polynomial approximations given to attach error bars.

ionizing EUV flux (see earlier). Points belonging to the solar cycle 24 (asterisks in Fig. 4, left panel) are inside  $\pm$  SD indicating no peculiarities in a comparison with other solar cycles. This also demonstrates Fig. 4 (right panel) where  $HL\alpha$  from the two cycles are compared using an enlarged scale. A linear approximation is applied for the two variations. This comparison confirms that the relationship between solar radio-emission and EUV should be the same in different solar cycles providing the observations are correct.

The  $CO_2$  cooling concept has been originated from model simulations by Roble and Dickinson (1989) and Rishbeth (1990) and is mainly supported by model simulations e.g. (Qian et al., 2008, 2011; Cnossen, 2014; Solomon et al., 2018, 2019). However the situation with first-principle models is not that straight. A comparison of various models with Millstone Hill ISR, CHAMP and COSMIC electron density observations (Shim et al., 2011, 2012) has shown that the empirical monthly median IRI model turns out to be one of the best. This does not mean that IRI is a very good model - it is not designed to describe particular geophysical conditions of a given day - but this tells us that modern 3D first-principle physical models are far from to be perfect. Similar results were obtained by Tsagouri et al. (2018) after a comparison of 3D physical to empirical models on the main ionospheric characteristics,  $f_oF_2$  and  $h_mF_2$ . Therefore, if 3D first-principle physical models are unable to describe with a sufficient accuracy the main ionospheric parameters such as  $f_oF_2$  and  $h_mF_2$  there is no certainty that long-term trends predicted with such models are correct bearing in mind that trends are very small - some percents per decade.

At present the only direct confirmation for cooling of the thermosphere provide satellite drag observations (see Introduction). We do not discuss the procedure how observed neutral gas density is recalculated into  $T_{ex}$  long-term trend when neutral composition is not known (this is done using thermospheric empirical models, see for instance, Emmert, 2015a), we only stress that such observations is the only experimental support for the thermospheric cooling. But satellite drag observations as this is discussed in our paper in fact do not quantitatively confirm the theoretically predicted magnitude of  $CO_2$  thermospheric cooling. The analyzed by Emmert (2015a) (1967–2013) period totally includes the falling phase (since middle of 1970s to 2008–2009) and namely this may be an explanation of negative  $\rho$  and  $T_{ex}$  trends obtained in his analysis. An extended analysis by Emmert et al. (2021) of satellite drag observations including the 2019 solar minimum seems to confirm the suggestion that we are entering into a new rising phase of solar activity as no decrease in neutral gas density (their Fig. 4) is seen in 2019 compared to 2008 solar minimum.

We are dealing with long-term trends in thermospheric rather than ionospheric parameters however it would be useful to mention ionospheric  $F_2$ -layer trends which directly manifest long-term trends in the

surrounding thermosphere. However there are many problems related to  $F_2$ -layer trends as this was mentioned in Introduction. According to Rishbeth (1977) “long-term changes can only be reliably detected over intervals of time that greatly exceed the 11-year solar cycle”. But long-term trends studies quite often use only 2 solar cycles (e.g. Laštovička et al., 2006; Danilov, 2008; Danilov and Konstantinova, 2013). Electron concentration in the  $F_2$ -layer crucially depends on many aeronomic parameters: solar EUV flux, neutral composition ( $O$ ,  $O_2$ ,  $N_2$ ) and temperature  $T_{ex}$ , thermospheric winds producing vertical plasma drifts. All of them may have their own long-term trends which are reflected in  $N_mF_2$  long-term variations. For instance, Danilov and Konstantinova (2014) were the first who have proposed to relate negative  $f_oF_2$  trends with the atomic oxygen decrease in the upper atmosphere and they prescribe this decrease to the intensification of eddy diffusion. Yes, daytime  $N_mF_2$  crucially depends on atomic oxygen concentration at  $F_2$ -layer heights but the long-term enhancement of poleward thermospheric wind (Mikhailov and Perrone, 2018) may be also responsible for  $f_oF_2$  negative trend at middle latitudes. Further any long-term intensification of eddy diffusion should result in general decrease of the atomic oxygen abundance in the upper atmosphere however our analysis (Perrone and Mikhailov, 2019) of column  $[O]$  long-term variations inferred from ionospheric observations has not revealed any statistically significant decrease in the column  $[O]$  abundance. It was shown that  $\sim 93\%$  of the whole  $[O]_{col}$  variability are explained by solar and geomagnetic activity long-term variations and only  $\sim 7\%$  may be attributed to other processes (reasons) including the anthropogenic impact. Therefore only a consistent analysis of long-term variations in the main aeronomic parameters responsible for the  $F_2$ -layer formation can provide an adequate explanation of the observed long-term changes in the ionospheric  $F_2$ -layer. Our method (Perrone and Mikhailov, 2018b) used in the present analysis provides such opportunity.

#### 4. Conclusions

The  $CO_2$  concentration has been increasing for more than five decades reaching  $\sim 29\%$  at present with respect to the pre-industrial era.  $CO_2$  cooling hypothesis predicts a noticeable decrease in thermospheric and ionospheric parameters especially under solar minimum conditions. The cooling concept needs a confirmation which is not easy to realize in practice. Our recently developed method by Perrone & Mikhailov, (2018b) provides this possibility at the quantitative level. A comparison of solar minima in 1954 and 1964 to other solar minima including the last one in 2019 with available ionospheric observations was used to check the theoretical predictions and the validity of the  $CO_2$  cooling hypothesis. June ionospheric observations at three European stations Moscow, Rome, and Slough/Chilton were used to infer neutral gas

density  $\rho$ , exospheric temperature  $T_{\text{ex}}$ , height of the F<sub>2</sub>-layer maximum  $h_m F_2$ , and total solar EUV flux for the (1954–2020) period. The obtained results may be formulated as follows.

1. Solar and geomagnetic activity was shown to explain ~99 % of the whole variability in the retrieved neutral gas density and  $T_{\text{ex}}$  during the (1958–2020) period. This 1 % of unexplained  $\rho$  variability is much less than an average decrease of 14.8 % in  $\rho$  expected from Solomon et al. (2018, 2019) model simulations for a 29 % CO<sub>2</sub> increase. The residual linear trends in  $\rho$ ,  $T_{\text{ex}}$ , and  $h_m F_2$  are statistically insignificant over the analyzed period.
2. A comparison of pre-industrial 1954 and 1964 solar minima to 2019 one when a quite visible decrease in thermospheric parameters is expected according to Solomon et al. (2018) model simulations does not confirm the predicted decrease of ~21 % in  $\rho$ , ~15 K in  $T_{\text{ex}}$ , and ~7 km in  $h_m F_2$  related to a 29 % increase in the CO<sub>2</sub> abundance.
3. The only direct experimental confirmation for the CO<sub>2</sub> cooling concept based on satellite drag observations (Emmert, 2015a, Table 2) gives only a ~5 K  $T_{\text{ex}}$  decrease over the analyzed period. This is much less than the CO<sub>2</sub> cooling hypothesis predicts. Therefore satellite drag observations in fact do not confirm at a quantitative level the CO<sub>2</sub> cooling concept.
4. The peculiarities with  $f_o F_2$  trends in the solar cycle 24 mentioned in the literature are not related to a distortion of the EUV versus F<sub>10.7</sub> dependence but presumably indicate the onset of a new rising phase in thermospheric and ionospheric parameter long-term variations after the deepest solar minimum in 2008/2009.
5. The main conclusion of the undertaken analysis: the origin of thermospheric and related to them ionospheric parameter long-term variations is natural rather than anthropogenic one as this was earlier suggested by Mikhailov and Marin (2000) and Perrone & Mikhailov (2016). Despite a continuous CO<sub>2</sub> increase in the Earth's atmosphere long-term variations of thermospheric parameter are controlled by solar and geomagnetic activity. The retrieved thermospheric parameters do not confirm the theoretically predicted decrease related to the CO<sub>2</sub> concentration increase in the Earth's upper atmosphere.

#### Declaration of competing interest

The authors declare that they have no known competing financial interests or personal relationships that could have appeared to influence the work reported in this paper.

#### Acknowledgements

The authors are grateful to T.N. Woods and his colleagues (<http://lasp.colorado.edu/lisird/>) for solar EUV observations data. Recent  $f_o F_2$  observations on Russian ionosonde stations are provided by Fedorov Institute of Applied Geophysics <http://ipg.geospace.ru/ionosphere-data-tables.html#31>. The Rome data are provided by Istituto Nazionale di Geofisica e Vulcanologia (<https://doi.org/10.13127/eswua/hf>). The authors thank the Lowell DIDBase through GIRO to provide ionospheric data (<http://giro.uml.edu/>). The authors thank: NOAA SWPC (<https://www.swpc.noaa.gov/>), GFZ Potsdam (<https://www.gfz-potsdam.de/en/kp-index/>) and the WDC for Geomagnetism, Kyoto (<http://wdc.kugi.kyoto-u.ac.jp/wdc/Sec3.html>) for geomagnetic indices ap and AE.

This work is supported by INGV-MUR (Ministry of University and Research), Italy Project Pianeta Dinamico - The Working Earth (CUP D53J19000170001), theme 3 SERENA."

#### References

Bremer, J., 1998. Trends in the ionospheric E and F regions over Europe. *Ann. Geophys.* 16, 986–996.

- Bremer, J., 2001. Trends in the thermosphere derived from global ionosonde observations. *Adv. Space Res.* 28, 997–1006.
- Bremer, J., 2008. Long-term trends in the ionospheric E and F1 regions. *Ann. Geophys.* 26, 1189–1197.
- Chamberlin, P.C., Woods, T.N., Eparvier, F.G., 2007. Flare irradiance spectral model (FISM): daily component algorithms and results. *Space Weather* 5, S07005. <https://doi.org/10.1029/2007SW000316>.
- Chapman, S., 1931. The absorption and dissociative or ionizing effect of monochromatic radiation in a atmosphere on a rotating Earth. *Proc. Roy. Soc. Lond.* 43 (1), 26–45, 43(5), 483–501.
- Cnossen, I., 2014. The importance of geomagnetic field changes versus rising CO<sub>2</sub> levels for long-term change in the upper atmosphere. *J. Space Weather Space Clim.* 4, A18.
- Danilov, A.D., 2006. Progress in studies of the trends in the ionospheric F region. *Phys. Chem. Earth* 31, 34–40.
- Danilov, A.D., 2008. Long-term trends in the relation between daytime and nighttime values of  $f_o F_2$ . *Ann. Geophys.* 26, 1199–1206.
- Danilov, A.D., 2012. Long-term trends in the upper atmosphere and ionosphere (a review). *Geomagn. Aeron.* 52, 338–347.
- Danilov, A.D., Konstantinova, A.V., 2013. Trends in the F2 layer parameters at the end of the 1990s and the beginning of the 2000s. *J. Geophys. Res. Atmos.* 118 <https://doi.org/10.1002/jgrd.50501>.
- Danilov, A.D., Konstantinova, A.V., 2014. Reduction of the atomic oxygen content in the upper atmosphere. *Geomagn. Aeron.* 54, 224–229.
- Danilov, A.D., Konstantinova, A.V., 2018. Long-term trends in the critical frequency of the E-layer. *Geomagn. Aeron.* 58, 338–347.
- Danilov, A.D., Konstantinova, A.V., 2019. Trends in  $f_o F_2$  and the 24th solar activity cycle. *Adv. Space Res.* 65, 959–965.
- Danilov, A.D., Konstantinova, A.V., 2020. Long-term variations in the parameters of the middle and upper atmosphere and ionosphere (review). *Geomagn. Aeron.* 60, 397–420.
- De Harro Barbas's, B.F., Ellias, A.G., 2019. Effect of the inclusion of solar cycle 24 in the calculation of  $f_o F_2$  long-term trend for Two/Japanese ionospheric stations. *Pure Appl. Geophys.* Springer Nature Switzerland AG. <https://doi.org/10.1007/s00024-019-02307-z>.
- Donaldson, J.K., Wellman, T.J., Oliver, W.L., 2010. Long-term change in thermospheric temperature above Saint Santin. *J. Geophys. Res.* 115, A11305. <https://doi.org/10.1029/2010JA015346>.
- Emmert, J.T., Dhady, M.S., Segerman, A.M., 2021. A Globally Averaged Thermospheric Density Data Set Derived from Two-Line Orbital Element Sets and Special Perturbations State Vectors. (accepted). <https://dx.doi.org/10.1029/2021JA029455>
- Emmert, J.T., Picone, J.M., Lean, J.L., Knowles, S.H., 2004. Global change in the thermosphere: compelling evidence of a secular decrease in density. *J. Geophys. Res.* 109, A02301. <https://doi.org/10.1029/2003JA010176>.
- Emmert, J.T., 2015a. Altitude and solar activity dependence of 1967–2005 thermospheric density trends derived from orbital drag. *J. Geophys. Res. Space Physics* 120, 2940–2950. <https://doi.org/10.1002/2015JA021047>.
- Emmert, J.T., 2015b. Thermospheric mass density: a review. *Adv. Space Res.* 56, 773–824.
- Jarvis, M.J., Jenkins, B., Rodgers, G.A., 1998. Southern hemisphere observations of a long-term decrease in F region altitude and thermospheric wind providing possible evidence for global thermospheric cooling. *J. Geophys. Res.* 103 (A9), 20,774–20,787.
- Keating, G.M., Tolson, R.H., Bradford, M.S., 2000. Evidence of long term global decline in the Earth's thermospheric densities apparently related to anthropogenic effects. *Geophys. Res. Lett.* 27, 1523–1526. <https://doi.org/10.1029/2000GL003771>.
- Laštovicka, J., 2013. Trends in the upper atmosphere and ionosphere: recent progress. *J. Geophys. Res. Space Physics* 118, 3924–3935. <https://doi.org/10.1002/jgra.50341>.
- Laštovicka, J., 2017. A review of recent progress in trends in the upper atmosphere. *J. Atmos. Sol. Terr. Phys.* 163, 2–13.
- Laštovicka, J., 2019. Is the relation between ionospheric parameters and solar proxies stable? *Geophys. Res. Lett.* 46 <https://doi.org/10.1029/2019GL085033>.
- Laštovicka, J., Mikhailov, A.V., Ulich, T., Bremer, J., Elias, A.G., Ortiz de Adler, N., Jara, V., Abarca del Rio, R., Foppiano, A.J., Ovalle, E., Danilov, A.D., 2006. Long-term trends in  $f_o F_2$ : A comparison of various methods. *J. Atmos. Sol. Terr. Phys.* 68, 1854–1870.
- Laštovicka, J., Solomon, S.C., Qian, L., 2012. Trends in the neutral and ionized upper atmosphere. *Space Sci. Rev.* 168, 113–145. <https://doi.org/10.1007/s11214-011-9799-3>.
- Machol, J., Snow, M., Woodraska, D., Woods, T., Viereck, R., Coddington, O., 2019. An improved Lyman-alpha composite. *Earth and Space Science* 6, 2263–2272. <https://doi.org/10.1029/2019EA000648>.
- Marcos, F.A., Wise, J.O., Kendra, M.J., Grossbard, N.J., Bowman, B.R., 2005. Detection of a long-term decrease in thermospheric neutral density. *Geophys. Res. Lett.* 32, L04103. <https://doi.org/10.1029/2004GL021269>.
- Mielich, J., Bremer, J., 2013. Long-term trends in the ionospheric F2 region with different solar activity indices. *Ann. Geophys.* 31, 291–303.
- Mikhailov, A.V., Skoblin, M.G., Förster, M., 1995. Day-time F2-layer positive storm effect at middle and lower latitudes. *Ann. Geophys.* 13, 532–540.
- Mikhailov, A.V., Marin, D., 2000. Geomagnetic control of the  $f_o F_2$  long-term trends. *Ann. Geophys.* 18, 653–665.
- Mikhailov, A.V., Marin, D., Leschinskaya, T.Yu., Herraiz, M., 2002. A revised approach to the  $f_o F_2$  long-term trends analysis. *Ann. Geophys.* 20, 1663–1675.



- Mikhailov, A.V., Perrone, L., Nusinov, A.A., 2017. A mechanism of midlatitude nighttime foE long-term variations inferred from European observations. *J. Geophys. Res. Space Physics* 122, 4466–4473. <https://doi.org/10.1002/2017JA023909>.
- Mikhailov, A.V., Perrone, L., 2018. Summer nighttime hmF2 long-term trends inferred from foF1 and foF2 ionosonde observations in Europe. *J. Geophys. Res.: Space Physics* 123. <https://doi.org/10.1029/2018JA025503>.
- Mikhailov, A.V., Perrone, L., 2020. Poststorm thermospheric NO overcooling? *J. Geophys. Res.: Space Physics* 125, e2019JA027122. <https://doi.org/10.1029/2019JA027122>.
- Nusinov, A.A., Katyushina, V.V., 1994. Lyman-alpha line intensity as a solar activity index in the far Ultraviolet Range. *Sol. Phys.* 152, 201–206. <https://doi.org/10.1007/BF01473205>.
- Nusinov, A.A., Kazachevskaya, T.V., Katyushina, V.V., 2021. Solar extreme and far ultraviolet radiation modeling for aeronomic calculations. *Rem. Sens.* 13 (2021), 1454. <https://doi.org/10.3390/rs13081454>.
- Ogawa, Y., Motoba, T., Buchert, S.C., Häggström, I., Nozawa, S., 2014. Upper atmosphere cooling over the past 33 years. *Geophys. Res. Lett.* 41, 5629–5635. <https://doi.org/10.1002/2014GL060591>.
- Oliver, W.L., Holt, J.M., Zhang, S.-R., Goncharenko, L.P., 2014. Long-term trends in thermospheric neutral temperature and density above Millstone Hill. *J. Geophys. Res. Space Physics* 119, 7940–7946. <https://doi.org/10.1002/2014JA020311>.
- Perrone, L., Mikhailov, A.V., 2016. Geomagnetic control of the midlatitude foF1 and foF2 long-term variations: recent observations in Europe. *J. Geophys. Res. Space Physics* 121, 7183–7192. <https://doi.org/10.1002/2016JA022715>.
- Perrone, L., Mikhailov, A.V., 2017. Long-term variations of exospheric temperature inferred from foF1 observations: a comparison to ISR Ti trend estimates. *J. Geophys. Res. Space Physics* 122, 8883–8892. <https://doi.org/10.1002/2017JA024193>.
- Perrone, L., Mikhailov, A.V., 2018a. Reply to comments by Zhang et al. on the paper “Long-term variations of exospheric temperature inferred from foF1 observations: a comparison to ISR Ti trend estimates” by Perrone and Mikhailov. *J. Geophys. Res.: Space Physics* 123. <https://doi.org/10.1029/2017JA025039>.
- Perrone, L., Mikhailov, A.V., 2018b. A new method to retrieve thermospheric parameters from daytime bottom-side Ne(h) observations. *J. Geophys. Res.: Space Physics* 123 (10). <https://doi.org/10.1029/2018JA025762>, 200–10,212.
- Perrone, L., Mikhailov, A.V., 2019. Long-term variations of June column atomic oxygen abundance in the upper atmosphere inferred from ionospheric observations. *J. Geophys. Res.: Space Physics* 124, 6305–6312. <https://doi.org/10.1029/2019JA026818>.
- Perrone, L., Mikhailov, A.V., Scotto, C., Sabbagh, D., 2020. Testing of the method retrieving a consistent set of aeronomic parameters with Millstone Hill ISR nighttime hmF2 observations. *Geosci. Rem. Sens. Lett. IEEE*. <https://doi.org/10.1109/LGRS.2020.3007362>.
- Qian, L., Solomon, S.C., Roble, R.G., Kane, T.J., 2008. Model simulations of global change in the ionosphere. *Geophys. Res. Lett.* 35, L07811. <https://doi.org/10.1029/2007GL033156>.
- Qian, L., Laštovička, J., Roble, R.G., Solomon, S.C., 2011. Progress in observations and simulations of global change in the upper atmosphere. *J. Geophys. Res.* 116, A00H03. <https://doi.org/10.1029/2010JA016317>.
- Qian, L., Burns, A.G., Solomon, S.C., Wang, W., 2017. Carbon dioxide trends in the mesosphere and lower thermosphere. *J. Geophys. Res. Space Physics* 122, 4474–4488. <https://doi.org/10.1002/2016JA023825>.
- Richards, P.G., Fennelly, J.A., Torr, D.G., 1994. EUVAC: a solar EUV flux model for aeronomic calculations. *J. Geophys. Res.* 99, 8981–8992.
- Rishbeth, H., 1990. A greenhouse effect in the ionosphere? *Planet. Space Sci.* 38, 945–948.
- Rishbeth, H., 1997. Long-term changes in the ionosphere. *Adv. Space Res.* 20, 2149–2155.
- Rishbeth, H., Roble, R.G., 1992. Cooling of the upper atmosphere by enhanced greenhouse gases – modelling of thermospheric and ionospheric effects. *Planet. Space Sci.* 40, 1011–1026.
- Roble, R.G., Dickinson, R.E., 1989. How will changes in carbon dioxide and methane modify the mean structure of the mesosphere and thermosphere? *Geophys. Res. Lett.* 16, 1441–1444.
- Roininen, L., Laine, M., Ulich, T., 2015. Time-varying ionosonde trend: case study of Sodankylä hmF2 data 1957–2014. *J. Geophys. Res. Space Physics* 120, 6851–6859. <https://doi.org/10.1002/2015JA021176>.
- Sharma, S., Chandra, H., Vyas, G.D., 1999. Long-term ionospheric trends over Ahmedabad. *Geophys. Res. Lett.* 26 (N3), 433–436.
- Shim, J.S., et al., 2011. CEDAR Electrodynamics Thermosphere Ionosphere (ETI) Challenge for systematic assessment of ionosphere/thermosphere models: NmF2, and hmF2, and vertical drift using ground-based observations. *Space Weather* 9, S12003. <https://doi.org/10.1029/2011SW000727>.
- Shim, J.S., et al., 2012. CEDAR Electrodynamics Thermosphere Ionosphere (ETI) Challenge for systematic assessment of ionosphere/thermosphere models: electron density, neutral density, NmF2, and hmF2 using space based observations. *Space Weather* 10, S10004. <https://doi.org/10.1029/2012SW000851>.
- Solomon, S.C., Liu, H.-L., Marsh, D.R., McInerney, J.M., Qian, L., Vitt, F.M., 2018. Whole atmosphere simulation of anthropogenic climate change. *Geophys. Res. Lett.* 45. <https://doi.org/10.1002/2017GL076950>.
- Solomon, S.C., Liu, H.-L., Marsh, D.R., McInerney, J.M., Qian, L., Vitt, F.M., 2019. Whole atmosphere climate change: dependence on solar activity. *J. Geophys. Res.: Space Physics* 124, 3799–3809. <https://doi.org/10.1029/2019JA026678>.
- Tsagouri, I., Goncharenko, L., Shim, J.S., Belehaki, A., Buresova, D., Kuznetsova, M.M., 2018. Assessment of current capabilities in modeling the ionospheric climatology for space weather applications: foF2 and hmF2. *Space Weather* 16, 1930–1945. <https://doi.org/10.1029/2018SW002035>.
- Ulich, Th., Turunen, E., 1997. Evidence for long-term cooling of the upper atmosphere in ionosonde data. *Geophys. Res. Lett.* 24 (N9), 1103–1106.
- Viereck, R., Puga, L., McMullin, D., Judge, D., Tobiska, K., 2001. The Mg II index: a proxy for solar EUV. *Geophys. Res. Lett.* 28 (N7), 1343–1346.
- Woods, T.N., Eparvier, F.G., Harder, J., Snow, M., 2018. Decoupling solar variability and instrument trends using the multiple same-irradiance-level (MuSIL) analysis technique. *Sol. Phys.* 293, 76. <https://doi.org/10.1007/s11207-018-1294-5>.
- Zhang, S.-R., Holt, J.M., Kurdzo, J., 2011. Millstone Hill ISR observations of upper atmospheric long-term changes: height dependency. *J. Geophys. Res.* 116, A00H05. <https://doi.org/10.1029/2010JA016414>.
- Zhang, S.-R., Holt, J.M., 2013. Long-term ionospheric cooling: dependency on local time, season, solar activity, and geomagnetic activity. *J. Geophys. Res.* 118, 3719–3730. <https://doi.org/10.1002/jgra.50306>.